Regular and Inverse Secondary Kinetic Enthalpy Effects (KHE) for the Rate of Inversion of Thioether and 1,1′-Biisoquinoline Complexes of Ruthenium and Osmium

Michael T. Ashby,* Susan S. Alguindigue, Justin D. Schwane, and Tad A. Daniel

Department of Chemistry and Biochemistry, The University of Oklahoma, 620 Parrington Oval, Rm. 208, Norman, Oklahoma 73019

Received May 30, 2001

Thioether complexes with the formula Δ/Λ-chloro(thioether)bis(2,2′-bipyridine)metal(II) (M = Ru, Os; thioether = dimethyl sulfide (**3a**$^+$), diethyl sulfide (**3b**$^+$), and tetrahydrothiophene (**3c**$^+$)) have been synthesized. The rates of inversion at the sulfur atom of the thioether ligands have been measured by spin-inversion transfer and line-shape NMR methods. In every case, the ruthenium derivative exhibits a faster inversion frequency at a given temperature than the corresponding osmium derivative. In contrast, similar complexes with the formula chloro-(*δ*/*λ*-1,1′-biisoquinoline)(2,2′:6′,2”-terpyridine)metal(II), **4(M=Ru,Os)**$^+$, undergo atropisomerization of the misdirected 1,1′-biisoquinoline (1,1′-biiq) ligand with rates that are faster for osmium than ruthenium. As a result of the lanthanide contraction effect and the similar metric parameters associated with the structures of second-row and third-row transition metal derivatives, steric factors associated with the isomerizations are presumably similar for the Ru and Os derivatives of these compounds. Since third-row transition metal complexes tend to have larger bond dissociation enthalpies (BDE) than their second-row congeners, we conclude the difference in reactivities of **3(M=Ru)**$^+$ versus **3(M=Os)**$^+$ and **4(M=Ru)**$^+$ versus **4(M=Os)**$^+$ are attributed to electronic effects. For **3**, the S3p lone pair of the thioether, the principal *σ* donor orbital, is orthogonal to the metal *σ* acceptor orbital in the transition state of inversion at sulfur and the S 3s orbital is an ineffective *σ* donor. Thus, a *regular relationship* between the kinetic and thermodynamic stabilities of **3(M=Ru)**$^+$ and **3(M=Os)**$^+$ is observed for the directed ⇌ [misdirected]‡ ⇌ directed (DMD) isomerization (the more thermodynamically stable bond is less reactive). In contrast, atropisomerization of **4**$^+$ involves redirecting (strengthening) the M−N bonds of the misdirected 1,1′-biiq ligand in the transition state. Therefore, an *inverse relationship* between the kinetic and thermodynamic stabilities of **4(M=Ru)**$^+$ and **4(M=Os)**$^+$ is observed for the misdirected ⇌ [directed]‡ ⇌ misdirected (MDM) isomerization (the more thermodynamically stable bond is more reactive). The rates obtained for **4**$^+$ are consistent with the rates of atropisomerization of Δ/Λ-(*δ*/*λ*-1,1′-biisoquinoline)bis(2,2′-bipyridine)-metal(II), **1(M=Ru,Os)**$^{2+}$, and (η^6-benzene) Δ/Λ-(*δ*/*λ*-1,1′-biisoquinoline)halometal(II), **2(M=Ru,Os;halo=Cl,I)**$^+$, that we reported previously. We term the relative rates of reaction of second-row versus third-row transition metal derivatives kinetic element effects (KEE = k_{second}/k_{third}). While the KEE appears to be generally useful when comparing reactions of isostructural species (e.g. the relative rates of **1(M=Ru)**$^{2+}$, **1(M=Os)**$^{2+}$, and **1-(M=Ir)**$^{3+}$), different temperature dependencies of reactions prevent the comparison of related reactions between species that have different structures (e.g., the 1,1′-biiq atropisomerization reactions of **1(M=Ru,Os)**$^{2+}$ versus **2(M=Ru,Os;halo=Cl,I)**$^+$ versus **4(M=Ru,Os)**$^+$). This problem is overcome by comparing entropies of activation and kinetic enthalpy effects (KHE = $\Delta H^‡_{third}/\Delta H^‡_{second}$). For a given class of 1,1′-biiq complexes, we observe a structure/reactivity relationship between $\Delta H^‡$ and the torsional twist of the 1,1′-biiq ligands that are measured in the solid state.

Introduction

We have previously determined that the mechanism of diastereomerization of Δ/Λ-(*δ*/*λ*-1,1′-biisoquinoline)bis(2,2′-bipyridine)metal(II), **1(M=Ru,Os)**$^{2+}$, proceeds via atropisomerization of the chiral 1,1′-biisoquinoline (1,1′-biiq) ligand rather than epimerization of the chiral metal center:[1−3]

We have suggested that the M−N bonds of the 1,1′-biiq ligand are bent in its ground state conformation and its donor orbitals are misdirected.[2−4] In the syn periplanar transition state

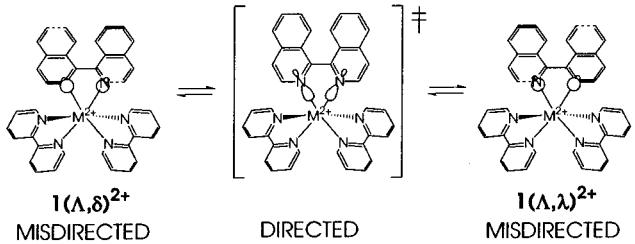

of the atropisomerization of **1**$^{2+}$, the nitrogen *σ* donor orbitals of the ligand are presumably more effectively directed at the *σ* acceptor orbitals of the metal as the M−N bonds of the 1,1′-biiq ligand are straightened.[3] Since third-row transition metals typically form stronger bonds than their second-row congeners,[5−15] the relatively more facile atropisomerization of **1(M=Os)**$^{2+}$ suggests the M−N bonds of the 1,1′-biiq ligand are weaker in

(1) Ashby, M. T.; Govindan, G. N.; Grafton, A. K. *Inorg. Chem.* **1993**, *32*, 3803.
(2) Ashby, M. T.; Govindan, G. N.; Grafton, A. K. *J. Am. Chem. Soc.* **1994**, *116*, 4801.
(3) Ashby, M. T. *J. Am. Chem. Soc.* **1995**, *117*, 2000.
(4) Ashby, M. T.; Alguindigue, S. S.; Khan, M. A. *Organometallics* **2000**, *19*, 547.

10.1021/ic0105720 CCC: $20.00
Published on Web 11/20/2001

the ground state than the transition state of the atropisomerization. Thus, an inverse relationship exists between the thermodynamic and kinetic stabilities of $\mathbf{1}^{2+}$ (the thermodynamically more stable derivative (Os) is kinetically more labile).[3] This same inverse relationship is observed for $\mathbf{2}^{+}$,[16] which is also believed to isomerize by a mechanism of atropisomerization of the 1,1′-biiq ligand:[4,16]

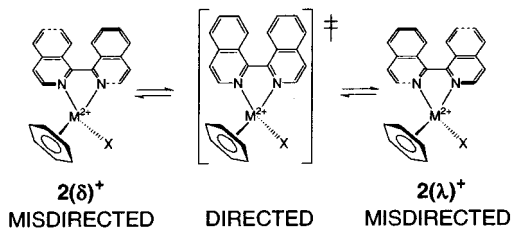

The linchpin of this structure/bonding/reactivity relationship is that Os−N bonds are stronger than Ru−N bonds, and this in turn should affect the lability of such bonds. Unfortunately, there are relatively few experimental data that compare the reaction kinetics and thermodynamics of identical second-row and third-row metal derivatives of complexes under the same conditions. Nonetheless, a general trend is observed whereby third-row transition metals form stronger bonds than their second-row congeners. A 2−54% increase in bond dissociation energies is observed for third-row compared to second-row transition metal complexes.[5−15] While it is expected on the basis of the usual trend that second-row transition metal−ligand bonds tend to be weaker than third-row transition metal−ligand bonds,[17] there is a potential danger in using kinetic lability as evidence of this trend. There are well-established examples of reactions for which decreased reactivity down a triad of transition metals is not observed,[18,19] novelties that are usually attributed to π-bonding effects for ligands such as carbon monoxide, solvent effects, or a change in mechanism.[20] Nonetheless, one generally observes a free-energy relationship between thermodynamic stability and kinetic inertness, particularly for simple σ-donor ligands. Because of the general paucity of available data, it would be desirable to compare the kinetics of simple ligand dissociation reactions of Ru and Os compounds. To bolster our hypothesis that a misdirected ⇌ [directed]‡ ⇌ misdirected (MDM) mechanism plays a role in determining the kinetics of the atropisomerization of $\mathbf{1}^{2+}$, we have synthesized a series of compounds, somewhat related to $\mathbf{1}^{2+}$, that undergo inversion at their thioether S-donor atoms via a directed ⇌ [misdirected]‡ ⇌ directed (DMD) mechanism: Δ/Λ-chloro(thioether)bis(2,2′-bipyridine)-metal(II), $\mathbf{3}^{+}$, e.g., where thioether = tetrahydrothiophene (THT):

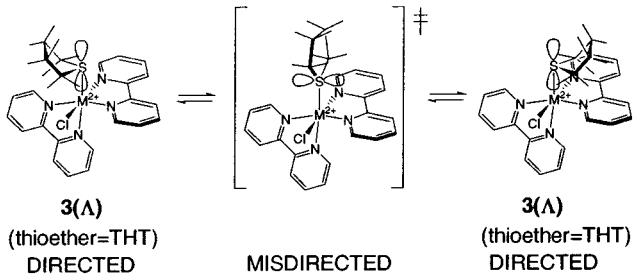

Since the M−S bond of $\mathbf{3}^{+}$ is stronger in the ground state than in the transition state (the opposite situation as compared with $\mathbf{1}^{2+}$ and $\mathbf{2}^{+}$), a regular kinetic relationship is expected whereby the thermodynamically more stable derivative should be kinetically less labile. Indeed, we find the second-row metal derivative of **3(M=Ru)**$^{+}$ is more labile than the third-row metal derivative **3(M=Os)**$^{+}$ with respect to inversion at the sulfur center.

In addition to our study of $\mathbf{3}^{+}$, we have sought out additional examples of atropisomerization of 1,1′-biiq to learn if the inverse free-energy relationship observed for $\mathbf{1}^{2+}$ and $\mathbf{2}^{+}$ is a general one. We report here the third example of an inverse free-energy relationship for a 1,1′-biiq complex, atropisomerization of chloro(δ/λ-1,1′-biisoquinoline)(2,2′:6′,2″-terpyridine)-metal(II), **4(M=Ru,Os)**$^{+}$:

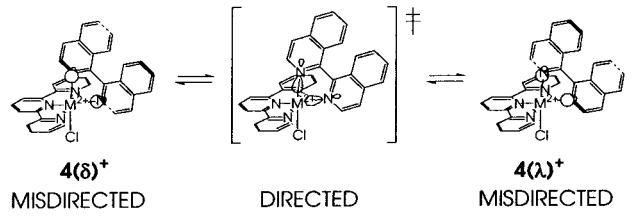

Once again, we observe an inverse free-energy relationship for the atropisomerization of a 1,1′-biiq complex with a faster rate for **4(M=Os)**$^{+}$ compared to **4(M=Ru)**$^{+}$.

Experimental Section

Absolute ethanol, acetonitrile, diethyl ether, the thioethers, and NH_4PF_6 were used as received. Dichloromethane-d_2 was dried over CaH_2 and distilled before use. Acetone-d_6 was used as received. $Ru(bipy)_2Cl_2$[21] and $Os(bipy)_2Cl_2$,[22] $Ru(terpy)Cl_3$,[23] $Os(terpy)Cl_3$,[24] and 1,1′-biiq[2] were synthesized using literature methods. ^{1}H NMR spectra were recorded on a Varian XL-500 using residual $CHDCl_2$ (5.32 ppm) and $OC(CD_3)(CHD_2)$ (2.04 ppm) as internal standards. The NMR samples were prepared in tubes that had been glass-blown onto Schlenk adapters. The solutions were freeze−pump−thawed, and the tubes were flame-sealed under vacuum.

General Procedure for the Synthesis of Δ/Λ-Chloro(thioether)-bis(2,2′-bipyridine)metal(II), 3(M=Ru,Os)$^{+}$. $M(bipy)_2Cl_2$ (M = Ru or Os, 0.3 mmol), absolute ethanol (8 mL), water (2 mL), and the thioether (5.0 mmol) were placed in a 50 mL Schlenk flask. The resulting solution was freeze−pump−thawed, left under vacuum, and

(5) Lewis, K. E.; Golden, D. M.; Smith, G. P. *J. Am. Chem. Soc.* **1984**, *106*, 3905.
(6) Li, J.; Schreckenbach, G.; Ziegler, T. *J. Am. Chem. Soc.* **1995**, *117*, 486.
(7) Ziegler, T.; Tschinkey, V.; Fan, L. Y.; Becke, A. D. *J. Am. Chem. Soc.* **1989**, *111*, 9177.
(8) Schock, L. E.; Marks, T. J. *J. Am. Chem. Soc.* **1988**, *110*, 7701.
(9) King, W. A.; DiBella, S.; Gulino, A.; Lanza, G.; Fragala, I. L. *J. Am. Chem. Soc.* **1999**, *121*, 355.
(10) Calhorda, M. J.; Dias, A. R.; Minas da Piedade, M. E.; Saleman, M. S.; Martinho Simões, J. A. *Organometallics* **1987**, *6*, 734.
(11) Tilset, M.; Parker, V. D. *J. Am. Chem. Soc.* **1989**, *111*, 6711.
(12) Ziegler, T.; Cheng, W.; Baerends, E.; Ravenek, W. *Inorg. Chem.* **1988**, *27*, 3458.
(13) Ziegler, T.; Tschinke, V.; Becke, A. *J. Am. Chem. Soc.* **1987**, *109*, 1351.
(14) Ziegler, T.; Tschinke, V.; Versluis, L.; Baerends, E. J. *Polyhedron* **1988**, *7*, 1625.
(15) Dias, A. R.; Martinho Simões, J. A. *Polyhedron* **1988**, *7*, 1531.
(16) Alguindigue, S. S.; Khan, M. A.; Ashby, M. T. *Organometallics* **1999**, *18*, 5112.
(17) Martinho Simões, J. A.; Beauchamp, J. L. *Chem. Rev.* **1990**, *90*, 629.
(18) Kettle, S. F. A. *Top. Curr. Chem.* **1977**, *71*, 71.
(19) Kirtley, S. W. In *Comprehensive Organometallic Chemistry*; Wilkinson, G., Stone, F. G. A., Abel, E. W., Eds.; Pergamon: Oxford, U.K., 1982; Vol. 3, pp 800−802.
(20) Ziegler, T.; Tschinke, V. *ACS Symp. Ser.* **1990**, *428*, 279−292.
(21) Sullivan, B. P.; Salmon, D. J.; Meyer, T. J. *Inorg. Chem.* **1978**, *17*, 3334.
(22) Kober, E. M.; Caspar, J. V.; Sullivan, B. P.; Meyer, T. J. *Inorg. Chem.* **1988**, *27*, 4587.
(23) Sullivan, B. P. *Inorg. Chem.* **1980**, *19*, 1404.
(24) Buckingham, D. A. *Aust. J. Chem.* **1964**, *17*, 622.

placed in an 80 °C oil bath. After 3 h, the Schlenk flask was connected via a T-adapter to another flask and the volume was reduced to approximately 2 mL (the ethanol was removed by vacuum transfer). All subsequent operations were carried out in the air. The resulting aqueous solution was filtered through a pipet containing Celite. The Celite column was washed with 2 mL of water. A 2 mL volume of water saturated with NH_4PF_6 was then added to the combined solutions to precipitate the product. The precipitate was collected on a fine frit and washed with cold water (2 × 10 mL) and diethyl ether (4 × 10 mL). The resulting solid was dried under high vacuum (10^{-5} Torr) for several hours. If the ^{1}H NMR spectrum revealed the presence of solvent or other impurities, the compound was recrystallized in the air, usually by vapor diffusion of diethyl ether into an acetonitrile solution of the compound. In all cases, fine powders and not well-defined single crystals of **3** were obtained. The one time that single crystals were obtained, it was after allowing the crystallization process to proceed much longer than usual, and in this case the crystals turned out to be $[Ru(bipy)_2(Cl)(NCCH_3)]PF_6$, which was presumably the result of decomposition.

Δ/Λ-Chloro(dimethyl sulfide)bis(2,2′-bipyridine)ruthenium(II) Hexafluorophosphate, 3a(M=Ru)PF$_6$. This was obtained as a red solid in 66% yield. Anal. Calcd (found) for $C_{22}H_{22}ClF_6N_4PRuS$: C, 40.28 (39.87); H, 3.38 (3.30). ^{1}H NMR (CD_2Cl_2, −40 °C, 500 MHz): δ 9.92 (d, 1H, J = 6 Hz); 9.56 (d, 1H, J = 6 Hz); 8.41 (d, 1H, J = 8 Hz); 8.34 (d, 1H, J = 8 Hz); 8.25 (m, 2H); 8.18 (m, 1H); 8.08 (m, 1H); 7.77−7.86 (m, 3H); 7.73 (m, 1H); 7.67 (d, 1H, J = 6 Hz); 7.46 (d, 1H, J = 5 Hz); 7.21 (m, 1H); 7.15 (m, 1H); 2.01 (s, 3H); 1.16 (s, 3H). Mass spectrum (FAB): m/z = 511 (M^+), 449 ($M^+ - C_2H_6S$).

Δ/Λ-Chloro(dimethyl sulfide)bis(2,2′-bipyridine)osmium(II) Hexafluorophosphate, 3a(M=Os)PF$_6$. This was obtained as a brown solid in 30% yield. Anal. Calcd (found) for $C_{22}H_{22}ClF_6N_4OsPS$: C, 35.75 (35.49); H, 3.00 (2.70). ^{1}H NMR (CD_2Cl_2, −50 °C, 500 MHz): δ 9.88 (d, 1H, J = 5 Hz); 9.44 (d, 1H, J = 6 Hz); 8.36 (d, 1H, J = 8 Hz); 8.32 (d, 1H, J = 8 Hz); 8.21 (m, 2H); 7.90 (m, 1H); 7.79 (m, 1H); 7.75 (m, 1H); 7.54−7.69 (m, 4H); 7.27 (d, 1H, J = 6 Hz); 7.10 (m, 1H); 6.96 (m, 1H); 2.00 (s, 3H); 1.25 (s, 3H). Mass spectrum (FAB): m/z = 601 (M^+), 539 ($M^+ - C_2H_6S$).

Δ/Λ-Chloro(diethyl sulfide)bis(2,2′-bipyridine)ruthenium(II) Hexafluorophosphate, 3b(M=Ru)PF$_6$. This was obtained as a red solid in 78% yield. Anal. Calcd (found) for $C_{24}H_{26}ClF_6N_4PRuS$: C, 42.51 (41.02); H, 3.87 (3.62). ^{1}H NMR (CD_2Cl_2, −80 °C, 500 MHz): δ 9.84 (d, 1H, J = 6 Hz); 9.58 (d, 1H, J = 5 Hz); 8.36 (m, 1H); 8.21 (m, 2H); 8.12 (m, 1H); 8.06 (m, 1H); 7.69−7.83 (m, 4H); 7.64 (d, 1H, J = 6 Hz); 7.38 (d, 1H, J = 5 Hz); 7.17 (m, 1H); 7.09 (m, 1H); 3.06 (dq, 1H, J = 14 Hz, J' = 7 Hz); 1.89 (dq, 1H, J = 14 Hz, J' = 7 Hz); 1.69 (dq, 1H, J = 14 Hz, J' = 7 Hz); 1.32 (dq, 1H, J = 14 Hz, J' = 7 Hz); 1.12 (m, 3H); 0.77 (t, 3H, J = 7 Hz). Mass spectrum (FAB): m/z = 539 (M^+), 449 ($M^+ - C_4H_{10}S$).

Δ/Λ-Chloro(diethyl sulfide)bis(2,2′-bipyridine)osmium(II) Hexafluorophosphate, 3b(M=Os)PF$_6$. This was obtained as a brown solid in 53% yield. Anal. Calcd (found) for $C_{24}H_{26}ClF_6N_4OsPS$: C, 37.57 (37.21); H, 3.42 (3.27). ^{1}H NMR (CD_2Cl_2, −60 °C, 500 MHz): δ 9.82 (d, 1H, J = 6 Hz); 9.48 (d, 1H, J = 5 Hz); 8.32 (t, 2H, J = 8 Hz); 8.18 (m, 2H); 7.85 (m, 1H); 7.77 (m, 1H); 7.72 (d, 1H, J = 6 Hz); 7.58−7.66 (m, 3H); 7.51 (m, 1H); 7.19 (d, 1H, J = 6 Hz); 7.07 (m, 1H); 6.91 (m, 1H); 3.00 (dq, 1H, J = 14 Hz, J' = 7 Hz); 1.94 (dq, 1H, J = 14 Hz, J' = 7 Hz); 1.77 (dq, 1H, J = 14 Hz, J' = 7 Hz); 1.49 (dq, 1H, J = 14 Hz, J' = 7 Hz); 1.12 (t, 3H, J = 7 Hz); 0.80 (t, 3H, J = 7 Hz). Mass spectrum (FAB): m/z = 629 (M^+), 539 ($M^+ - C_4H_{10}S$).

Δ/Λ-Chloro(tetrahydrothiophene)bis(2,2′-bipyridine)ruthenium(II) Hexafluorophosphate, 3c(M=Ru)PF$_6$. This was obtained as a red solid in 88% yield. Anal. Calcd (found) for $C_{24}H_{24}ClF_6N_4PRuS$: C, 42.27 (41.97); H, 3.55 (3.51). ^{1}H NMR (CD_2Cl_2, −50 °C, 500 MHz): δ 9.86 (d, 1H, J = 6 Hz); 9.76 (d, 1H, J = 6 Hz); 8.38 (d, 1H, J = 9 Hz); 8.32 (d, 1H, J = 9 Hz); 8.25 (d, 1H, J = 8 Hz); 8.21 (d, 1H, J = 8 Hz); 8.12 (t, 1H, J = 8 Hz); 8.06 (t, 1H, J = 8 Hz); 7.68−7.82 (m, 5H); 7.38 (d, 1H, J = 5 Hz); 7.18 (t, 1H, J = 7 Hz); 7.11 (t, 1H, J = 7 Hz); 3.24 (m, 1H); 2.89 (m, 1H); 2.06 (m, 1H); 1.75 (m, 1H); 1.61 (m, 1H); 1.02 (m, 2H); 0.92 (m, 1H). Mass spectrum (FAB): m/z = 537 (M^+), 448 ($M^+ - C_4H_8S$).

Δ/Λ-Chloro(tetrahydrothiophene)bis(2,2′-bipyridine)osmium(II) Hexafluorophosphate, 3c(M=Os)PF$_6$. This was obtained as a brown solid in 86% yield. Anal. Calcd (found) for $C_{24}H_{24}ClF_6N_4OsPS$: C, 37.38 (37.11); H, 3.14 (3.05). ^{1}H NMR (CD_2Cl_2, −50 °C, 500 MHz): δ 9.81 (m, 1H); 9.64 (m, 1H); 8.33 (m, 2H); 8.20 (d, 1H, J = 7 Hz); 7.79−7.85 (m, 3H); 7.60−7.67 (m, 3H); 7.53 (m, 1H); 7.21 (m, 1H); 7.08 (m, 1H); 6.93 (m, 1H); 3.20 (m, 1H); 2.87 (m, 1H); 2.03 (m, 1H); 1.77 (m, 1H); 1.63 (m, 1H); 1.18 (m, 2H); 1.01 (m, 1H). Mass spectrum (FAB): m/z = 627 (M^+), 539 ($M^+ - C_4H_8S$).

Synthesis of Chloro(δ/λ-1,1′-biisoquinoline)(2,2′:6′,2″-terpyridine)ruthenium(II) Chloride, 4(M=Ru)Cl. Ru(terpy)Cl_3 (160 mg, 0.36 mmol), 1,1′-biiq (160 mg, 0.62 mmol), lithium chloride (80 mg, 1.9 mmol), triethylamine (0.8 mL), and 75% aqueous ethanol (150 mL) were placed in a 250 mL round-bottom flask. The resulting suspension was heated to reflux and stirred vigorously for 4 h. The solution was then cooled and filtered using a medium frit. The frit was washed with ethanol (3 × 10 mL), and the combined filtrate were concentrated to approximately 15 mL using a rotary evaporator during which time the complex precipitated out of solution as a deep purple solid. The product was isolated by filtration using a medium frit, washed with distilled water (2 × 10 mL), recrystallized by vapor diffusion of diethyl ether into an acetonitrile solution, and dried under a high vacuum (10^{-5} Torr) for several hours to give a dark purple powder (180 mg, 75%). ^{1}H NMR (CD_2Cl_2, 30 °C, 500 MHz): δ 10.44 (d, 1H, J = 6 Hz); 8.69 (br d, 1H); 8.64 (br d, 1H); 8.49 (br t, 2H); 8.36 (d, 1H, J = 6 Hz); 8.29 (d, 1H, J = 8 Hz); 8.20 (br, 1H); 8.11 (d, 1H, J = 9 Hz); 8.01 (d, 1H, J = 9 Hz); 7.95−7.81 (m, 5H); 7.68 (m, 2H); 7.57 (m, 2H); 7.30 (br, 1H); 7.11 (t, 1H, J = 6 Hz); 7.06 (t, 1H, J = 6 Hz); 6.82 (d, 1H, J = 6 Hz). Mass spectrum (FAB): m/z = 626 (M^+).

Synthesis of Chloro(δ/λ-1,1′-biisoquinoline)(2,2′:6′,2″-terpyridine)osmium(II) Chloride, 4(M=Os)Cl. Os(terpy)Cl_3 (200 mg, 0.38 mmol), 1,1′-biiq (200 mg, 0.78 mmol), and ethylene glycol (5 mL) were placed in a 50 mL Schlenk tube. The resulting solution was freeze−pump−thawed, left under vacuum, and placed in a 198 °C oil bath for 90 min. The volatiles were removed by vacuum transfer, the residue was dissolved in acetonitrile, the solution was filtered, and the acetonitrile was removed on a rotary evaporator. The resulting solid was chromatographed on grade I basic alumina, eluting with acetonitrile. The third band was collected, the volatiles were removed using a rotary evaporator, and the complex was recrystallized by vapor diffusion of diethyl ether into an acetonitrile solution to give dark purple crystals (13 mg, 6%). ^{1}H NMR (CD_2Cl_2, 20 °C, 500 MHz): δ 10.32 (d, 1H, J = 6 Hz); 8.50 (d, 1H, J = 8 Hz); 8.45 (d, 1H, J = 8 Hz); 8.29 (br d, 2H, J = 6 Hz); 8.24 (d, 1H, J = 8 Hz); 8.18 (dd, 1H, J = 8 Hz, J' = 2 Hz); 8.06 (m, 2H); 7.78−7.72 (m, 2H); 7.69−7.59 (m, 4H); 7.54 (m, 3H); 7.22 (d, 1H, J = 6 Hz); 7.11 (d, 1H, J = 6 Hz); 7.02 (m, 2H); 6.83 (d, 1H, J = 5 Hz). Mass spectrum (FAB): m/z = 716 (M^+).

Symmetry of Magnetic Exchange by 2D EXSY. The two-dimensional exchange spectroscopy (2D EXSY) pulse sequence and the experimental procedure used to carry out these experiments have been described in detail elsewhere.[4,25] The spectrum of Figure 1 for **3b(M=Os)**$^+$ only illustrates the positive peaks; therefore, the cross-peaks corresponding to chemical exchange are observed. Similar spectra were obtained for all of the compounds.

Rates of Thioether Inversion by Spin-Inversion Transfer (SIT) NMR. SIT rate data were obtained using the standard pulse sequence[26−29] and methods that have been described previously.[16] Typical fits for spin transfer and inversion recovery are illustrated in Figure S2. The rate constants that were derived from the SIT experiments and the conditions that were employed for each experiment are summarized in Table 1.

Rates of Atropisomerization by NMR Line-Shape Analysis (LSA). It was possible to measure the rates of thioether inversion of **3b**$^+$ and atropisomerization of **4**$^+$ by LSA. LSA was carried out using

(25) Abel, E. W.; Coston, T. P. J.; Orrell, K. G.; Sik, V.; Stephenson, D. *J. Magn. Reson.* **1986**, *70*, 34.
(26) Alger, J. R.; Prestegard, J. H. *J. Magn. Reson.* **1977**, *27*, 137.
(27) Kuchel, R. W.; Chapman, B. E. *J. Theor. Biol.* **1983**, *105*, 569.
(28) Bellon, S. F.; Chen, D.; Johnston, E. R. *J. Magn. Reson.* **1987**, *73*, 168.
(29) Robinson, G.; Kuchel, P. W.; Chapman, B. E. *J. Magn. Reson.* **1985**, *63*, 314.

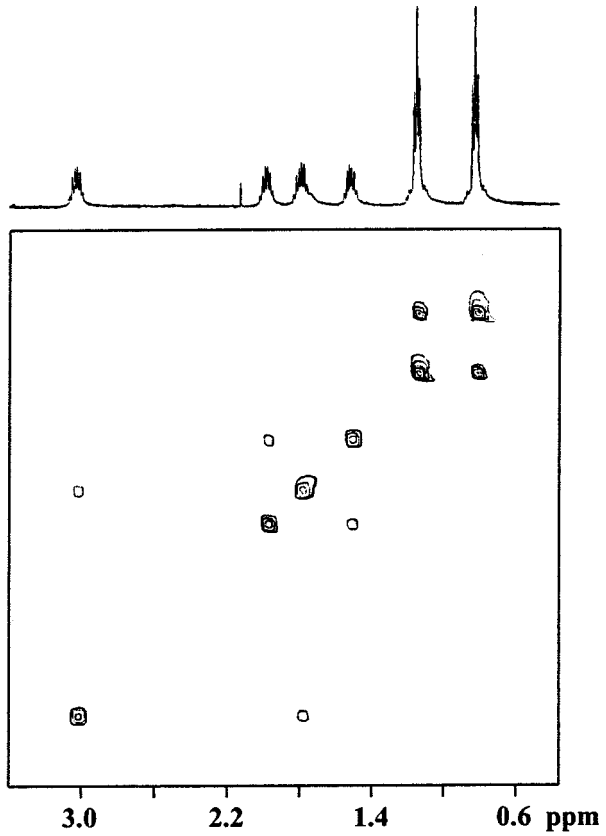

Figure 1. 2D-EXSY NMR spectrum for **3b(M=Os)**$^+$ at 213 K and 500 MHz that illustrates pairwise chemical exchange.

Table 1. Kinetic Parameters Obtained by SIT for Inversion of the Thioether Ligands of **3a−c(M=Ru,Os)**$^+$ in CD_2Cl_2

compd	thioether	T (°C)	k (s^{-1})	$\Delta G^{\ddagger}$ (kJ mol^{-1})
3a(M=Ru)$^+$	Me_2S	−40	14.4(2)	52
3a(M=Os)$^+$	Me_2S	−20	8.0(3)	57
3b(M=Ru)$^+$	Et_2S	−80	4.4(1)	44
3b(M=Os)$^+$	Et_2S	−60	3.75(6)	49
3c(M=Ru)$^+$	C_4H_8S	−50	17(2)	49
3c(M=Os)$^+$	C_4H_8S	−50	1.9(4)	53

Table 2. Kinetic Data Obtained by LSA for Inversion of the Thioether Ligands of **3b(M=Ru)**$^+$ and **3b(M=Os)**$^+$ in Acetone-d_6

temp (°C)	M = Ru k (s^{-1})	M = Os k (s^{-1})	KEE
−90	2.189(6)	0.0046(1)	476
−85	4.09(1)		
−80	6.80(2)	0.0183(8)	372
−70	22(1)	0.10(7)	22
−60	53.0(3)	0.461(2)	115
−40	249(6)	4.54(3)	55
−20		31.1(3)	

the FORTRAN program DNMR5 running on a Silicon Graphics IRIS Indigo X24.[30] The rate constants that were derived from the LSA, and the conditions that were employed for each experiment are summarized in Table 2 for compound **3b(M=Ru,Os)**$^+$ and Table 3 for compound **4(M=Ru, Os)**$^+$.

X-ray Crystal Structure of 4(M=Os)$^+$Cl$^-$·H$_2$O. A Siemens P4 four-circle diffractometer[31] was used to collect a $\theta/2\theta$ data set at 173-(2) K using Mo Kα radiation (0.710 73 Å). The data were corrected for Lorentz and polarization effects, and an empirical absorption correction based on ψ-scans was applied.[32] The structure was solved by the heavy atom method using the Siemens SHELXTL system and refined by full-matrix least squares of F^2 using all of the reflections.[33] All of the non-hydrogen atoms were refined anisotropically, and all of the hydrogen atoms were included in the refinement at geometrically idealized positions with fixed temperature factors except the hydrogen atoms belonging to a disordered H_2O solvent molecule. The asymmetric unit contains a **4(M=Os)**$^+$ cation, a Cl^- anion, and a disordered water molecule. Crystallographic solution and refinement procedures, atomic coordinates, anisotropic displacement parameters, and hydrogen coordinates are listed in the Supporting Information. Selected interatomic distances, angles, and torsion angles are given in Table 4. A diagram illustrating the thermal ellipsoids at the 50% level of the molecule and the labeling scheme are shown in Figure 2.

Table 3. Kinetic Data Obtained by LSA for Atropisomerization of **4(M=Ru)**$^+$ and **4(M=Os)**$^+$ in CD_2Cl_2

temp (°C)	M = Ru k (s^{-1})	M = Os k (s^{-1})	KEE
20		0.469(2)	
30	0.07(1)		
40		2.8(2)	
50	0.66(2)	6.3(1)	0.11
60	1.6(6)	13.8(7)	0.12
70	3.9(3)	28.73(5)	0.14
80	9.0(2)	58.9(3)	0.15
85	13.2(2)		
90	19.7(3)	108.8(2)	0.18
95	27.7(4)		
100	42.3(7)	201(1)	0.21

Table 4. Comparison of Selected Interatomic Distances (Å), Angles (deg), and Torsion Angles (deg) for **4(M=Ru,Os)**$^+$ [a]

Ru−N(1)	2.072(4)	Os−N(1)	2.063(4)
Ru−N(2)	2.029(4)	Os−N(2)	2.031(4)
Ru−N(3)	2.050(4)	Os−N(3)	2.055(4)
Ru−N(4)	1.952(4)	Os−N(4)	1.975(4)
Ru−N(5)	2.075(4)	Os−N(5)	2.056(4)
RuCl	2.420(1)	OsCl	2.402(1)
N(1)−Ru−N(2)	77.5(2)	N(1)−Os−N(2)	77.3(1)
N(3)−Ru−N(4)	80.1(2)	N(3)−Os−N(4)	79.7(2)
N(3)−Ru−N(5)	159.6(2)	N(3)−Os−N(5)	159.0(2)
N(4)−Ru−N(5)	79.7(2)	N(4)−Os−N(5)	79.3(2)
N(1)−C(9)−C(10)−N(2)	22.7(6)	N(1)−C(9)−C(10)−N(2)	21.1(6)
N(3)−C(23)−C(24)−N(4)	6.5(6)	N(3)−C(23)−C(24)−N(4)	5.8(6)
N(4)−C(28)−C(29)−N(5)	2.0(6)	N(4)−C(28)−C(29)−N(5)	3.0(6)

[a] Note the labeling scheme for **4(M=Ru)**$^+$ has been changed from that originally published[56] to make it conform to the scheme of Figure 2. Also, the content of the asymmetric units of the two structures are not the same: **4(M=Ru)$^+$ClO$_4^-$·MeCN** versus **4(M=Os)$^+$Cl$^-$·H$_2$O**.

Results and Discussion

Directed ⇌ [Misdirected]‡ ⇌ Directed (DMD) Inversion of Thioether Complexes. The rates of inversion at thioethers have been previously investigated for a wide range of metal complexes.[34] We sought to make a comparison between the rates of second- and third-row derivatives analogous to the previously studied complexes of 1,1′-biiq−**1**$^{2+}$, $[M(bipy)_2(biiq)]^{2+}$ (M = Ru, Os).[2,3] Accordingly, we synthesized the thioether complexes **3**$^+$, $[M(bipy)_2(Cl)(SR_2)]^+$ (M = Ru, Os), using a method that has been used to synthesize similar complexes of other classes of neutral donor ligands; e.g., $[M(bipy)_2(Cl)(DMSO)]^+$,[35] $[M(bipy)_2(Cl)(acetone)]^+$,[36] and $[M(bipy)_2(Cl)(pyridine)]^+$.[37]

(30) Stephenson, D. S.; Binsch, G. *QCPE 365. DNMR5: Iterative Nuclear Magnetic Resonance Program for Unsaturated Exchange-Broadened Band shapes*; Institute of Organic Chemistry, University of Munich: Munich, FRG, 1978.
(31) *Siemens XCSANS: X-ray single-Crystal Analysis System*, version 2.1; Siemens Analytical X-ray Instruments Inc.: Madison, WI, 1994.
(32) North, A. C. T.; Phillips, D. C.; Mathews, F. S. *Acta Crystallogr.* **1968**, *A24*, 351.
(33) *SHELXTL Software Package for the Determination of Crystal Structures*, release 5.1; Siemens Analytical X-ray Instruments, Inc.: Madison, WI, 1995.
(34) Abel, E. W.; Bhargava, S. K.; Orrell, K. G. *Prog. Inorg. Chem.* **1984**, *32*, 1.

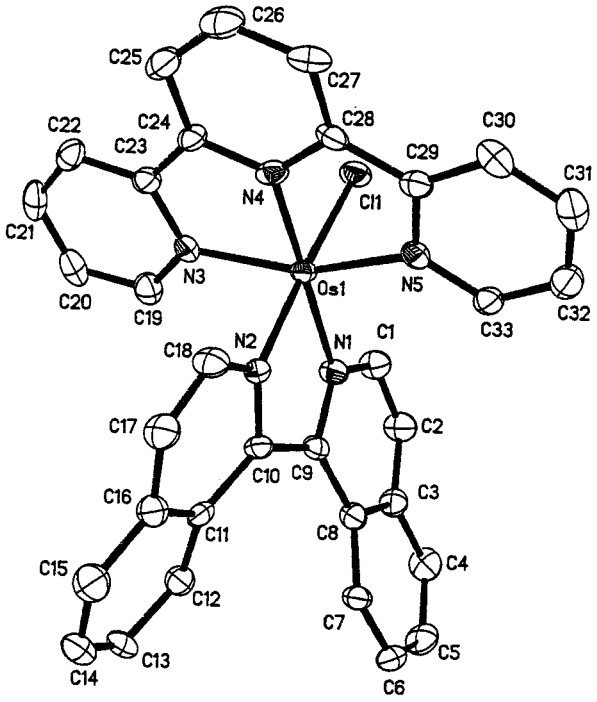

Figure 2. Molecular structure of **4(M=Os)**$^+$ showing the atom-labeling scheme and the thermal vibration ellipsoids (50% probability).

The normally insoluble complexes $[M(bipy)_2Cl_2]$ (M = Ru,-Os) dissolve in hot aqueous alcohol to produce homogeneous solutions, presumably of the aquated metals.[38] Addition of thioethers to such solutions give monosubstituted products. FAB mass spectra of **3c(M=Ru,Os)**$^+$ confirm that the chloride ion is coordinated to the metal. Operationally, it is convenient to add an excess of the thioether to the reaction mixture before heating. We have not observed the formation of bis(thioether) complexes under these reaction conditions. Attempts to synthesize more highly substituted analogues of **3** with isopropyl sulfide and *tert*-butyl sulfide failed. Parenthetically, we were successful in synthesizing a derivative of the unsymmetrical sulfide thioanisole. The thioanisole derivative bears two chiral centers, the metal and the sulfur, and therefore exists as diastereomers in a ratio of ca. 10:1 (M = Ru). The relatively large equilibrium constant makes the measurement of accurate rate constants by NMR spin-labeling methods difficult. Furthermore, although we did not synthesize the compound, the osmium derivative would likely have a different equilibrium ratio of the two diastereomers (cf. **1(M=Ru,Os)**$^{2+}$ and the explanation for a difference in diastereomeric thermodynamics),[3] and this would complicate a direct comparison of the rate constants of the ruthenium and osmium derivatives; therefore, we focused on symmetrical thioether derivatives for the purpose of this study.

Given the chiral nature of the metal center of **3**$^+$ and the pyramidal geometry of the sulfur center, the two R groups of the thioether are diastereotopic. Figure 1 illustrates a representative 2D EXSY spectrum for the derivative **3b(M=Os)**$^+$ at −60 °C. At this temperature, the ^{1}H NMR spectrum of **3b(M=Os)**$^+$ is static rendering all four of the methylene protons and the two methyl groups magnetically inequivalent. The off-diagonal peaks of the spectrum clearly demonstrate that chemical exchange takes place on the spin-relaxation time scale even though chemical exchange is slow on the time scale of the NMR experiment. Interconversion of the ^{1}H NMR signals of the thioether ligand indicates either inversion at the sulfur, inversion at the metal center, or complete dissociation of the thioether ligand. Low-spin d^6 derivatives of group 8 metals (e.g. **1**$^{2+}$ and **3**$^+$) are known to be stereochemically stabile at the metal centers,[39] and in the present case the 2D EXSY spectra illustrate this experimentally. If the metal center were stereochemically fluxional on the time scale of the 2D EXSY experiment, there would be off-diagonal peaks in the bipyridine region of the spectrum (region not shown in Figure 1).[40] Furthermore, the fact that off-diagonal peaks between free and coordinated thioether ligands are not observed when excess thioether is added to the sample (also not shown in Figure 1) demonstrates that exchange between free and coordinated thioether ligands is not taking place on the time scale of the 2D EXSY experiment. Finally, the spectrum of Figure 1 clearly illustrates pairwise exchange of the protons; exchange of all four methylene protons would be expected if the thioether ligand was dissociating from the metal. Therefore, we conclude the dynamic process is intramolecular inversion at the thioether ligand.

Following the collection of 2D EXSY spectra to determine the symmetry of exchange, spin-inversion transfer (SIT) data were collected for **3a−c(M=Ru,Os)**$^+$. Ideally, these data would have been collected over a wide, overlapping temperature range so that enthalpic and entropic contributions to the S inversion barriers could be separated (vide infra). After measuring such data for **3c(M=Ru,Os)**$^+$, we concluded that the quality of the data precluded the accurate determination of $\Delta H^{\ddagger}$ and $\Delta S^{\ddagger}$. Furthermore, the temperature range over which rate constants could be determined was rather narrowly bound at low temperature by the effective competition of the rate of chemical exchange with respect to the rate of spin−lattice relaxation and at high temperature by the coalescence temperature, the temperature at which the NMR spectrum becomes dynamic. In some cases the freezing point of the solvent also became an issue. Unfortunately, only in the case of **3c** was it possible to determine the rate constants at the same temperature for the Ru and Os derivatives by SIT. Thereafter, we simply measured the rates at the temperature at which the spectrum just becomes static, conditions under which the rate of chemical exchange is as large as possible with respect to the rate of spin−lattice relaxation. These data are summarized in Table 1. A representative fit of SIT data is illustrated in Figure S2 for **3c(M=Ru)**$^+$. It was possible to collect rate data over a large temperature range (−20 °C to −90 °C) for **3b(M=Ru,Os)**$^+$, albeit in a different solvent, using LSA. These data are summarized in Table 2. The same fluxional behavior was observed in acetone as in methylene chloride. The activation parameters that were calculated from the rate data for compound **3b(M=Ru,Os)**$^+$ are summarized in Table 5.

Before discussion of the results we have obtained for the thioether inversion frequencies of **3**, the nature of the bonding between the metal and the sulfur atom of a thioether ligand deserves comment. Hybridization of the valence orbitals of divalent chalcogenides is not important beyond the second

(35) Birchall, J. D.; O'Dinoghne, T. D.; Wood, J. R. *Inorg. Chim. Acta* **1979**, *37*, L461.
(36) Adeyemi, S. A.; Millar, F. J.; Meyer, T. J. *Inorg. Chem.* **1972**, *11*, 994.
(37) Sullivan, B. P.; Salmon, D. J.; Meyer, T. J.; Peedin, J. *Inorg. Chem.* **1979**, *18*, 3369.
(38) Dwyer, F. P.; Goodwin, H. A.; Gyarfas, E. C. *Aust. J. Chem.* **1963**, *16*, 544.
(39) Wilkins, R. G. *Kinetics and Mechanism of Reactions of Transition Metal Complexes*; VCH: Weinheim, Germany, 1991; p 355.
(40) The only mechanism for epimerization of the metal center that would not give rise to off-diagonal peaks in the 2D EXSY spectrum would involve an unreasonable hexagonal planar transition state.

Table 5. Comparison of Thermodyamic Data, Kinetic Element Effects (KEE), and Kinetic Entropy Effects (KHE) for Atropisomerization of 1,1′-Biisoquinoline (1,1′-biiq), Ethyl Sulfide, and 1,1′-Biphenyl-2,2′-diamine (dabp) Complexes of Ruthenium and Osmium in Acetone-d_6

	compd	$\Delta H^{\ddagger}$ (kJ/mol)	$\Delta S^{\ddagger}$ (J/K mol)	$\Delta G_{50}^{\ddagger}$ (kJ/mol) (50 °C)	KEE (50 °C)	KHE	ref
1(M=Ru)$^{2+}$	$[Ru(bipy)_2(1,1\text{-biiq})]^{2+}$ [a]	68(2)	−33(4)	78.7			2
1(M=Os)$^{2+}$	$[Os(bipy)_2(1,1\text{-biiq})]^{2+}$ [a]	65(2)	−24(5)	72.8			3
	$[M(bipy)_2(1,1\text{-biiq})]^{2+}$ [b]				0.13	0.96	
2(M=Ru,X=Cl)$^{+}$	$[(\eta^6\text{-}C_6H_6)Ru(1,1\text{-biiq})(Cl)]^{+}$	77.3(2)	4.8(7)	75.7			4
2(M=Os,X=Cl)$^{+}$	$[(\eta^6\text{-}C_6H_6)Os(1,1\text{-biiq})(Cl)]^{+}$	71.2(2)	−11.6(7)	74.9			4
	$[(\eta^6\text{-}C_6H_6)M(1,1\text{-biiq})(Cl)]^{+}$				0.74	0.92	
2(M=Ru,X=I)$^{+}$	$[(\eta^6\text{-}C_6H_6)Ru(1,1\text{-biiq})(I)]^{+}$	76.5(3)	−5(1)	78.1			4
2(M=Os,X=I)$^{+}$	$[(\eta^6\text{-}C_6H_6)Os(1,1\text{-biiq})(I)]^{+}$	70.2(5)	−21(1)	77.0			4
	$[(\eta^6\text{-}C_6H_6)M(1,1\text{-biiq})(I)]^{+}$				0.60	0.92	
3b(M=Ru)$^{+}$	$[Ru(Et_2S)(terpy)(Cl)]^{+}$	32.5(1)	−56.6(5)	50.8			e
3b(M=Os)$^{+}$	$[Os(Et_2S)(terpy)(Cl)]^{+}$	46.2(1)	−31.9(5)	56.5			e
	$[M(Et_2S)(terpy)(Cl)]^{+}$				22*c*	1.42	
4(M=Ru)$^{+}$	$[Ru(1,1\text{-biiq})(terpy)(Cl)]^{+}$	80.4(6)	0(1)	80.4			e
4(M=Os)$^{+}$	$[Os(1,1\text{-biiq})(terpy)(Cl)]^{+}$	66.2(1)	−25.2(2)	74.3			e
	$[M(1,1\text{-biiq})(terpy)(Cl)]^{+}$				0.11	0.82	
5(M=Ru)$^{+}$	$[(\eta^6\text{-}C_6H_6)Ru(dabp)(Cl)]^{+}$			66.8			16
5(M=Os)$^{+}$	$[(\eta^6\text{-}C_6H_6)Os(dabp)(Cl)]^{+}$			65.3			16
	$[(\eta^6\text{-}C_6H_6)M(dabp)(Cl)]^{+}$				0.51[d]		

[a] The values shown correspond to the interconversion of the minor ⟶ major diastereomerization. [b] KEE and KHE are an average of minor ⟶ major and major ⟶ minor diastereomerization reactions. [c] Measured at −70 °C. [d] Measured at 20 °C. [e] This study.

period.[41] Thus, the lone pair of a thioether ligand may be viewed as essentially unhybridized atomic orbitals.[41,42] One of the lone pair is an out-of-plane S 3p orbital (of b_1 symmetry in the C_{2v} point group), and the other is essentially a S 3s orbital (of a_1 symmetry in the C_{2v} point group), albeit mixed somewhat with a higher-energy orbital (also of a_1 symmetry) that is strongly bonding in nature. The out-of-plane S 3p lone pair is the principal σ-donor orbital of a thioether ligand, as evidenced by the acute "tilt angles" (the angle between the plane containing the R_2S moiety and the M−S vector).[43,44] The tilt angles of thioether complexes approach 90°, whereas the tilt angles of corresponding ethers range from nearly 90 to 180°. The s-type lone pair of a thioether ligand is an ineffectual donor as compared with the p-type lone pair. This is due largely to the diffuse nature of the S s-orbital and the fact that it is somewhat bonding in character. The transition state for inversion at the S atom of a thioether ligand (with its trigonal planar geometry at sulfur) involves a substantially weakened M−S bond. Thus, a significant barrier exists for inversion at the S atom of a thioether ligand. In the context of the present study, inversion at the S atom may be viewed as a directed ⇌ [misdirected]‡ ⇌ directed (DMD) process with respect to the M−S bond.

The barriers for inversion at the thioether ligands of **3**$^{+}$ range from 44 to 57 kJ/mol, which are in the range that have been measured for other thioether−metal complexes, 28 kJ/mol being the smallest[45] and 81 kJ/mol the largest[46] barrier we have encountered for simple thioether ligands. Most significant with respect to main objective of this study, we find in all cases for a given thioether derivative of **3**$^{+}$ the frequency of inversion at the sulfur atom is more rapid for the Ru derivative as compared with the Os derivative at a given temperature. The trend we observe with respect to the steric demand of the thioether R groups is also worthy of comment. Abel et al. have measured the inversion barriers at sulfur for *cis*-$[Mo(CO)_4(RSCH_3CH_2SR)]$ and found the trend for $\Delta G^{\ddagger}$ to be $CH_3 > CH_2CH_3 > CH(CH_3)_2 > C(CH_3)_3$.[47] The authors quite reasonably attribute this trend to a relief of steric strain upon changing the geometry at sulfur from pyramidal to trigonal planar. We note a similar trend for **3**$^{+}$; e.g., $\Delta G^{\ddagger}$(**3a(M=Ru)**$^{+}$) > $\Delta G^{\ddagger}$(**3b(M=Ru)**$^{+}$). Although it was not pointed out in their report, we note for $[Mo(CO)_4(RSCH_3CH_2SR)]$ the trend in $\Delta H^{\ddagger}$ is $CH_3 > CH_2CH_3 > CH(CH_3)_2 > C(CH_3)_3$, but the trend in $\Delta S^{\ddagger}$ is $CH_3 < C(CH_3)_3 < CH_2CH_3 < CH(CH_3)_2$. We have previously discussed the significance of the order of $\Delta S^{\ddagger}$.[48,49]

Misdirected ⇌ [Directed]‡ ⇌ Misdirected (MDM) Isomerization of 1,1′-Biisoquinoline Complexes. Comparison of the rates of isomerization of the Ru and Os derivatives of $[M(bipy)_2(1,1'\text{-biiq})]^{2+}$, **1**$^{2+}$, has led to introduction of the term kinetic element effect (KEE),[4] the ratio of the rates of isomerization reactions of second-row and third-row metal−ligand complexes (KEE = k_{second}/k_{third}). The KEE may be compared to kinetic isotope effects (KIE). The sign of a secondary KIE can give information concerning the transition-state of the reaction (e.g., whether the secondary bond is strengthened or weakened). The KEE is related to the KIE because of lanthanide contraction.[50] Similar to the relationship between hydrogen and deuterium, second-row and third-row transition metals are the same size with different masses and bond energetics.[51] The different bond dissociation energies of second-row and third-row transition metals give rise to an opportunity to explore bond strength without changing the steric effects in a system. Therefore, comparison of rates of second-row and third-row transition metal isomerization reactions that do not involve the breaking of bonds can give information concerning the transition states of these reactions. In the context of misdirected ligands, rates of isomerization reactions that perturb metal−ligand bonds can be used to compare relative ground-state versus transition-state metal−ligand bond energies. A KEE that is greater than one is indicative of a weakening of the metal−ligand bonds in the

(41) Kutzelnigg, W. *Angew. Chem., Int. Ed. Engl.* **1984**, *23*, 272.
(42) Ashby, M. T.; Sheshtawy, N. A. *Organometallics* **1994**, *3*, 236.
(43) Ashby, M. T. Dissertation, University of Arizona, 1986.
(44) Ashby, M. T. *Comments Inorg. Chem.* **1990**, *10*, 297.
(45) Eekhof, J. H.; Hogeveen, H.; Kellogg, R. M.; Klei, D. *J. Organomet. Chem.* **1978**, *161*, 183.
(46) Abel, E. W.; Bhargava, S. K.; Kite, K.; Orrell, K. G.; Sik, V.; Williams, B. L. *Polyhedron* **1982**, *1*, 289.
(47) Abel, E. W.; Budgen, D. E.; Moss, I.; G., O. K.; Sik, V. *J. Organomet. Chem.* **1989**, *362*, 105.
(48) Das, P. K.; Alguindigue, S. S.; Ashby, M. T. *Can. J. Chem.* **2001**, *79*, 809.
(49) Ashby, M. T.; Alguindigue, S. S.; Khan, M. A. *Inorg. Chim. Acta* **1998**, *270*, 227.
(50) Huheey, J. E.; Huheey, C. L. *J. Chem. Educ.* **1972**, *49*, 227−30.
(51) Ohanessian, G.; Goddard, W. A., III. *Acc. Chem. Res.* **1990**, *23*, 386.

transition state, while a KEE of less than one suggests a strengthening of bonds in the transition state.

An inverse KEE is observed for the 1,1′-biiq ligand complexes $[M(bipy)_2(1,1'\text{-biiq})]^{2+}$,[3] $[(\eta^6\text{-}C_6H_6)M(1,1'\text{-biiq})(Cl)]^+$,[4] $[(\eta^6\text{-}C_6H_6)M(1,1'\text{-biiq})(I)]^+$,[4] and $[M(1,1'\text{-biiq})(terpy)(Cl)]^+$ and the dabp ligand complex $[(\eta^6\text{-}C_6H_6)M(dabp)(Cl)]^+$ (M = Ru, Os).[16] The magnitude of the KEE varies for the various 1,1′-biiq compounds (Table 5). It is interesting that the KEE is similar in magnitude for the arene−metal−chloride versus −bromide complexes, $\mathbf{2}^+$, but very different for the bis(bipyridine) complexes, $\mathbf{1}^{2+}$. It appears that the ancillary ligands may influence the magnitude of the KEE. The faster kinetic rates that are observed for the osmium derivative of the dabp complex, $\mathbf{5}^+$, suggests that the inverse relationship between thermodynamic stability and kinetic lability is not a special property of the 1,1′-biiq ligand but could be a general trend for complexes with misdirected metal−ligand bonds.

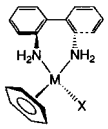

$\mathbf{5(\delta)}^+$

Kinetic Enthalpy Effect (KHE). The rightmost columns of Tables 2 and 3 illustrate a problem associated with using the KEE to elucidate mechanisms. We have frequently encountered a significant difference in the entropies of activation ($\Delta S^{\ddagger}$) for second-row metal derivatives compared to their third-row congeners,[4] and this in turn produces a temperature dependency of the KEE. Similar temperature effects are observed for KIE, but the affects are generally less pronounced.[52,53] Although we have not encountered a case where the inclination of the KEE was reversed at different temperatures, we can avoid this potential problem by comparing the enthalpies of activation ($\Delta H^{\ddagger}$) rather than rate constants. Furthermore, $\Delta H^{\ddagger}$ is directly related to bond strength.[54,55] We define the ratio of enthalpy of activation between the third-row and second-row transition metal complexes as the kinetic enthalpy effect (KHE = $\Delta H^{\ddagger}_{third}/\Delta H^{\ddagger}_{second}$). Note, in contrast to the KEE, we have employed the parameter of the heavy element in the numerator of the quotient that defines KHE so as to maintain the usual definitions of regular and inverse effects (cf. KIE). Since third-row bonds of ground states are generally stronger than second-row bonds, and this trend presumably translates to related transition states, a regular KHE would be observed when KHE > 1, while an inverse effect is observed when KHE < 1. An inverse KHE is observed for each of the 1,1′-biiq ligand systems (Table 5). It was not possible to calculate the KHE for $[(\eta^6\text{-}C_6H_6)M(dabp)(Cl)]^+$ because enthalpic and entropic contributions could not be separated for the osmium complex.[16] It is remarkable that the KHE's for $\mathbf{1}^{2+}$, $\mathbf{2}^+$, and $\mathbf{4}^+$ are comparable.

Structure/Reactivity Relationship for Metal Complexes of 1,1′-Biisoquinoline. We have determined the crystal structure of $\mathbf{4(M{=}Os)}^+$ to compare it to the structure of its Ru derivative (Table 4).[56] Most significant is the fact that the only metric parameters that are significantly different for the two structure are those associated with the nonplanarity of the 1,1′-biiq ligands. We have noted a general relationship between the extent to which the 1,1′-biiq ligand is twisted and the observed barriers of atropisomerization. Now that we have collected structural and thermokinetic data for seven complexes of 1,1′-biiq, we can begin to quantify the relationship. Figure 3 plots the enthalpies of activation versus torsion angles (Table 6) for these complexes. Figure 3 clearly illustrates, for a given class of compounds (e.g., $\mathbf{1}^{2+/3+}$, $\mathbf{2}^+$, or $\mathbf{4}^+$), the osmium derivative exhibits a more acute N−C−C′−N′ torsion angle and lower enthalpy of activation. Furthermore, for the case where we have three isostructural derivatives ($\mathbf{1(M{=}Ru)}^{2+}$, $\mathbf{1(M{=}Os)}^{2+}$, and $\mathbf{1(M{=}Ir)}^{3+}$ [57]), there appears to be a linear relationship between the torsional angle and enthalpic activation barrier. This result is a manifestation of the Hammond postulate: transition states begin to resemble ground states for low-barrier transformations, and vice-versa.[58]

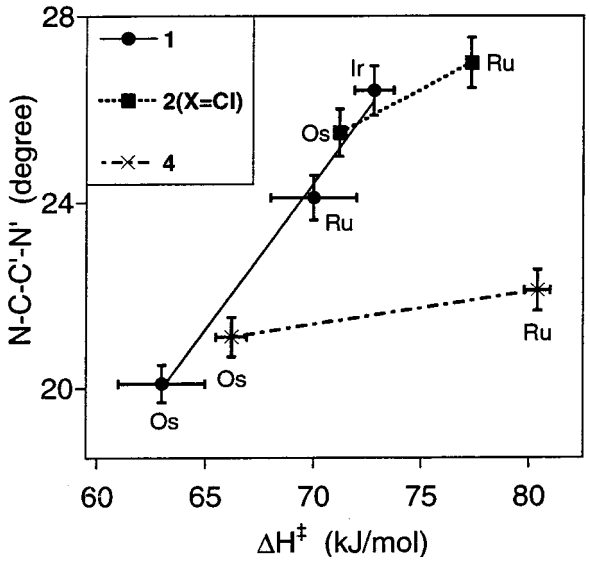

Figure 3. Relationship between the N−C−C′−N′ torsional angles of various metal−biisoquinoline complexes and their enthalpies of activation for atropisomerization. For $\mathbf{2(X{=}Cl)}^+$ and $\mathbf{4}^+$, tie lines are drawn that connect the two data points of each; however, the line that connects the derivatives of **1** is the result of least-squares analysis. Note the data for $\mathbf{1(M{=}Ir)}^{3+}$ are unpublished results.[57]

Table 6. Comparison of Torsion Angles (deg) and Activation Enthalpies (kJ mol^{-1}) for 1,1′-Biisoquinoline Complexes of Ruthenium and Osmium

compd	N−C−C′−N′	$\Delta H^{\ddagger}$ (kJ mol^{-1})	ref
$[Ru(bipy)_2(biiq)]^{2+}$	−24.1(6)	68(2)	2
$[Os(bipy)_2(biiq)]^{2+}$	−20.1(1)	65(2)	3
$[(\eta^6\text{-benzene})Ru(biiq)(Cl)]^+$	27.0(2)	77.3(2)	4
$[(\eta^6\text{-benzene})Os(biiq)(Cl)]^+$	25.5(4)	71.2(2)	4
$[Ru(biiq)(terpy)(Cl)]^+$	22.1(5)	80.4(6)	56
$[Os(biiq)(terpy)(Cl)]^+$	21.1(5)	66.2(7)	this study

Conclusion

The rates of inversion at the sulfur atom of a series of compounds $[M(bipy)_2(Cl)(thioether)]^+$, $\mathbf{3(M = Ru, Os)}^+$, have been measured by spin-labeling NMR methods. In every case, the ruthenium derivative exhibits a faster inversion frequency at a given temperature than the corresponding osmium derivative. Therefore, a *regular relationship* between the kinetic and thermodynamic stabilities of $\mathbf{3(M{=}Ru)}^+$ and $\mathbf{3(M{=}Os)}^+$ is

(52) Scheiner, S. *Biochim. Biophys. Acta* **2000**, *1458*, 28.
(53) Kwart, H. *Acc. Chem. Res.* **1982**, *15*, 401.
(54) Ribeiro Da Silva, M. A. V. *New J. Chem.* **1997**, *21*, 671.
(55) Mortimer, C. T. *NATO ASI, Ser. C* **1984**, *119*, 289−315.
(56) Yu, W.-Y.; Cheng, W.-C.; Che, C.-M.; Wang, Y. *Polyhedron* **1994**, *13*, 2963.
(57) Ashby, M. T.; Manke, I. A.; Khan, M. A. Unpublished results.
(58) Hammond, G. S. *J. Am. Chem. Soc.* **1955**, *77*, 334.

observed for the directed ⇌ [misdirected]‡ ⇌ directed (DMD) isomerization (the more thermodynamically stabile bond is less reactive). This contrasts with the rates of atropisomerization of the 1,1′-biiq ligands of chloro(δ/λ-1,1′-biisoquinoline)(2,2′:6′,2″-terpyridine)metal(II), **4(M=Ru,Os)**$^+$, which undergo misdirected ⇌ [directed]‡ ⇌ misdirected (MDM) isomerizations that exhibit an *inverse relationship* between their kinetic and thermodynamic stabilities (the more thermodynamically stabile bonds are more reactive). These conclusions are supported by the *regular* kinetic enthalpy effect (KHE = $\Delta H^{\ddagger}_{third}/\Delta H^{\ddagger}_{second}$) of 1.42 that was measured for **3b**$^+$ compared with the *inverse* KHE's that were determined for **1**$^{2+}$, **2**$^+$, and **4**$^+$ of 0.96, 0.92, and 0.82, respectively.

Acknowledgment. The financial support of the Petroleum Research Fund (PRF No. 29900-AC3) and the National Science Foundation (Grant CHE-9612869) is gratefully acknowledged. J.D.S. (1997) and T.A.D (1998) were National Science Foundation Summer Undergraduate Research Fellows (CHE-9531538). S.S.A. was a Department of Education GAANN Fellow.

Supporting Information Available: Tables of crystal and structure refinement data, atomic coordinates and equivalent isotropic displacement parameters, bond lengths and angles, anisotropic displacement parameters, hydrogen coordinates and isotropic displacement parameters, and torsion angles and crystal packing diagram for **4(M=Os)**$^+$**Cl**$^-$**·H$_2$O**, a SIT fit and LSA of **3b(M=Ru)**$^+$, an Eyring plot for LSA of **3b(M=Ru)**$^+$ and **3b(M=Os)**$^+$, and an X-ray crystallographic file for **4(M=Os)**$^+$**Cl**$^-$**·H$_2$O**, in CIF format. This material is available free of charge via the Internet at http://pubs.acs.org.

IC0105720